MORPHOLOGY OF STRUCTURAL DOMAINS
IN A CONGRUENTLY ORDERED $L1_0$ PHASE Fe-Pd ALLOY

B. Cheong and D. E. Laughlin
Department of Materials Science and Engineering
Carnegie Mellon University, Pittsburgh, PA 15213

Introduction

Atomic ordering of a disordered *fcc* phase into the $L1_0$ phase is accompanied by a reduction in point group symmetry as well as in translational symmetry (Fm3m ---> P4/mmm). The reduction in point group symmetry renders three rotational modifications (or three crystallographic *variants*) of the $L1_0$ phase; in terms of spatial regions, this results in three kinds of *structural domains*. An important point here is that each of the structural domains is distorted along its own tetragonal axis and, thus, the $L1_0$ single phase is an aggregate of the domains of three different distortion directions. Under this circumstance, the relative volume fraction of the variants, the habit plane between structural domains and the shape of a structural domain plate, which constitute essential features of the microstructures of the $L1_0$ phase, can not be arbitrary, but are subject to the systematics governed by minimization of the elastic strain energy. In this report, we discuss a few characteristics of these morphological features, as observed in thin (<100 µm) specimens of $L1_0$ single phase Fe-Pd alloys.

Experimental Procedure

As-cast buttons of the Fe-45.1 at.% Pd alloy were provided by the Lawrence Livermore National Laboratory. The buttons were initially given a homogenization treatment of 3 days at 1150 °C. Subsequently, they were sliced into pieces, with thicknesses of about 0.5 mm, and were cold-rolled to a thickness of about 0.2 mm. After being subject to an intermediate anneal of 10 min at 1150 °C, the specimens were finally cold-rolled into sheets, with thicknesses of less than 0.1 mm. The sheet specimens were then given a disordering treatment for 15 min at 1150 °C. In each of the above heat treatments, the specimens were encapsulated in argon back-filled quartz tubes and heated in a box furnace, which was maintained at a temperature, controlled to an accuracy of ±3 °C. Quenching of the disordered specimens was carried out by rapidly transferring the quartz tubes to iced-brine water and smashing them onto a heavy metal object, which was immersed in the quenchant. Aging of the quenched specimens was performed in a three zone tube furnace, with specimens encapsulated in argon back-filled pyrex tubes. The aged specimens were washed in hydrochloric acid, diluted with water, and discs of 3 mm in diameter were prepared therefrom. The disc specimens were electro-polished, using a twin-jet electro-polisher with an electrolyte of 82 vol.% acetic acid, 9 vol.% perchloric acid and 9 vol.% ethanol at a temperature of 3 °C and a potential of 17 V. Electron microscopy was conducted, using a Philips 420T microscope as well as a JEOL 120 CX, both operating at 120 kV.

Results and Discussions

A) Development of Microstructure and the Variant Volume Fraction

The quenched disordered alloys were aged at 450 °C for various times. TEM photographs, taken from an alloy aged for 2 min are shown in Fig. 1a). From the SADP, one can notice broad and diffuse superlattice intensity, uniformly distributed over three different variants (marked by arrows). Consistent with this, the DF image shows small ordered domains of sizes about 1 - 3 nm which are more or less randomly dispersed throughout the matrix. Slightly longer aging of the quenched alloy produced conspicuously different features. This is shown in Fig. 1b), taken from a 5 min aged state. From the SADP, it is found that the superlattice reflections are now much stronger and sharper and that the fundamental reflections display noticeable splitting (marked by an arrow in the SADP). This indicates that the tetragonal lattice distortion of the $L1_0$ ordered domains increased with the enhancement of long range order. In conjunction with this, one can notice from the DF image, regular arrays of growing ordered domains, which are aligned along the $\langle 011 \rangle_{fcc}$ directions. It is known that this particle alignment is a manifestation

of the elastic strain energy minimization, resulting from the strain-induced elastic interaction among tetragonal strain centers (1,2). An interesting feature in the SADP regarding the constitution of the microstructure is the non-uniform distribution of the intensity of superlattice reflections among 3 different crystallographic variants. This suggests that the spatial rearrangement of the ordered domains into the regular arrays is accompanied by a change in the relative volume fraction of different variants.

With further aging, the ordered domains grow and coalesce to gradually develop an $L1_0$ single phase state. The resulting single phase microstructures are shown in the DF image of Fig. 1c), taken from an alloy aged for 48 h. From the associated SADP, one can notice that the intensity of superlattice reflections is now markedly non-uniform among the 3 variants, and is, indeed, distributed primarily over two variants. These two variants are denoted as B and C in the SADP; A is mainly due to double diffraction. Consistent with this, the DF image shows alternating bright and dark domains of two variants. The boundaries between two neighboring structural domains of different variants are found to be along the <011> directions. The predominance of the two variant state was consistently observed in alloys aged under the same conditions. Yet, the relative volume fraction of two different variants was found to change, depending on the local region of a specimen. The $L1_0$ single phase state of an alloy, aged at 480 °C for 19 h after aging at 450 °C for 60 h is shown in Fig. 1d). As compared with the single phase microstructures shown in Fig. 1c), a few changes may be noticed. Most prominently, the microstructure now consists, overwhelmingly, of one variant, suggesting that a transition from a two variant state to a single variant state is taking place. This may be seen, for example, in the serrated boundaries between the two variants, which
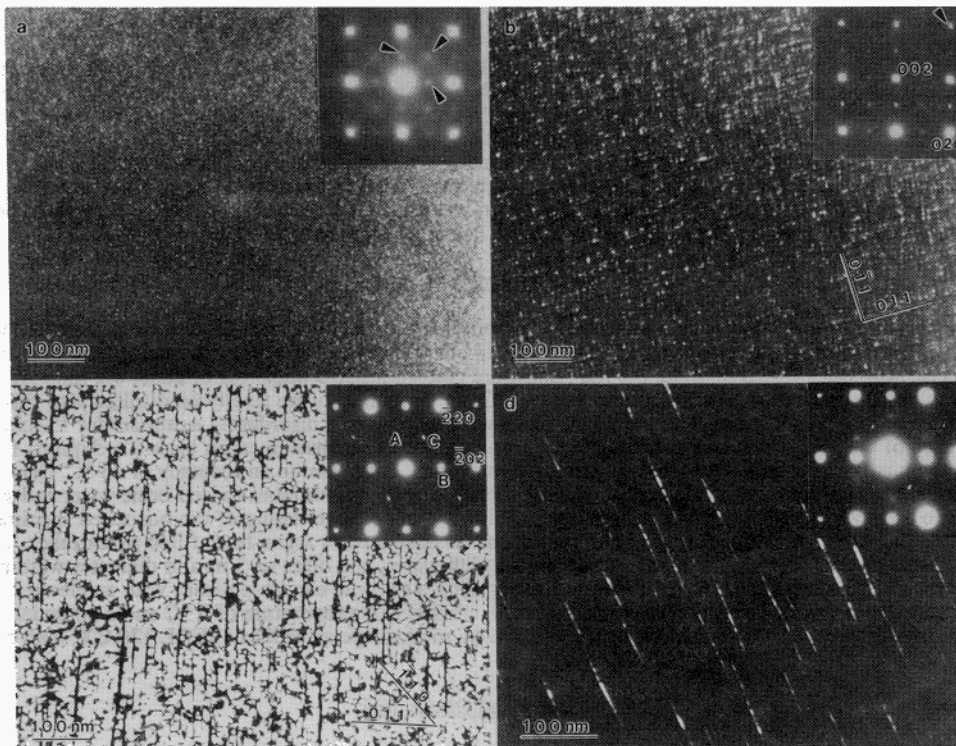

Figure.1: SADP's and the DF images using superlattice reflections which describe the sequential development of the microstructures during congruent $L1_0$ ordering of the Fe-45at.%Pd alloys: aged at 450°C for (a) 2 min, (b) 5 min, (c) 48 h, and (d) aged at 450 °C for 60 h followed by aging at 480 °C for 19h. Notice a sequential transition in variant volume fraction from three to two to near single variant.

appear to be in the process of conversion of a structural domain of one kind to the other. This near single variant state was more frequently observed than it was in alloys aged at 450 °C. It should be stated that the aged alloys discussed above have displayed a common macroscopic phenomenon, that is, buckling of the specimen. This was found to occur after a certain stage of aging and became more pronounced as aging progressed in the $L1_0$ single phase state.

The general trend displayed in Fig. 1 with regard to the change in the relative volume fraction of the structural domains is interesting. This sequential transition of a three to two to one variant has been observed in a few other experimental studies of lower temperature $L1_0$ ordering using thin specimens (3,4). However, little discussion and explanation have been provided. In order to gain a qualitative understanding, we first review the prediction of elasticity theories of polytwin-domain morphology (5-7). According to the theories, in a phase transformation involving a *fcc* to *fct* crystal structure change, a complete elimination of the volume dependent elastic strain energy due to the homogeneous transformation strain is made possible by the formation of a polytwin domain complex in which domains of different variants alternate with specific volume fractions. The equilibrium volume fraction (z_0), which ensures a complete relaxation of the elastic strain energy (or satisfying the condition of *invariant plane strain*), is given by

$$z_0 = \frac{\varepsilon_{33}^o}{\varepsilon_{33}^o - \varepsilon_{11}^o} \tag{1}$$

where ε_{11}^o and ε_{33}^o are the components of the stress free transformation strain tensor. It can be seen from the equation that, unless $\varepsilon_{11}^o = -\varepsilon_{33}^o$, the volume fractions of two different variants in a stress free state can not be equal to each other. When the lattice parameters of the equiatomic Fe-Pd alloy (8) are used ($\varepsilon_{11}^o \approx -0.636\ \varepsilon_{33}^o$), z_0 is calculated to be about 0.61 for the major variant.

Although the volume fraction analysis, provided by the theories, renders some insight, it explains no more than a general trend, namely, the predominance of a two variant state. This is mainly because the transformation mode premised in the theories differs from that of the $L1_0$ ordering we observed in the Fe-45at.%Pd alloy. The analysis may be strictly valid when a transformation proceeds by a heterogeneous mode in which a system under transformation remains a heterogeneous mixture of both a parent phase and a product phase for most of the reaction time. In this case, the morphology of the transformed regions of a product phase would be such that it accommodates the transformation strain under the constraint imposed by the untransformed matrix of a parent phase. This seems to explain why higher temperature ordering reactions, characterized by a rapid growth of a small number of nuclei, are often found to lead to the microstructures which are in good agreement with the theoretical predictions (9).

Unlike the situation treated in the theories, the $L1_0$ ordering in the Fe-Pd alloy was found to proceed uniformly throughout the whole specimen, involving a cooperative growth of a large number of nuclei. Since the parent *fcc* phase virtually disappears after the initial stages of ordering, during the subsequent ordering process, accommodation of the transformation strain in a local region of a specimen is subject to the constraint due to its surroundings, which are also in the process of ordering. Under these circumstances, the variant volume fraction in a local region would certainly be different from that predicted by eq. (1). Furthermore, the volume fraction would continuously change if the stress state of the surroundings changes with the progress of ordering. The adjustment of the variant volume fraction would remain an important means to relax the volume dependent elastic strain energy, as long as an ordering region is substantially constrained. If the constraining ability of the surroundings diminishes, an ordering region would tend to transform to a single variant state, which satisfies the total free energy minimum in the stress free state. This may explain why transition to a near single variant state is more frequently observed as buckling of the specimen becomes pronounced.

B) Shape of a Structural Domain Plate

The $L1_0$ single phase microstructures, shown above, are the prototypical ones, which clearly depict plate-like regions of two different variants bounded by the {110} habit planes. In many cases, however, we found microstructures display markedly different features, depending on the orientations of the plates relative to the direction of observation. In fact, one can utilize this aspect to study the shape of a structural domain plate. The $L1_0$ single phase microstructures shown in Fig. 2 were taken near the [110] zone axis from an alloy aged at 450 °C for 48 h. A characteristic feature of the SADP is the absence of superlattice reflections. Consistent with this, we see no APB contrast in the BF micrograph. As illustrated in the schematic diagram, these features may only be expected when the region under examination contains two variants with their c axes at a respective angle of 45° with the

[110] foil orientation. In the BF image, the structural domains of the minor variant are delineated by the loop contrast, distributed throughout the matrix of the major variant. The semi-axes of the loops are found to lie along the [1$\bar{1}$0] direction (long axis) and the [001] direction (short axis).
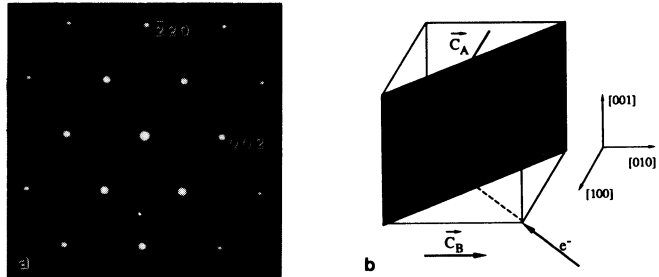

Figure 2:

Single $L1_0$ phase microstructure taken along the [110] zone axis from an alloy aged at 450 °C for 48 h. (a) [110] zone axis SADP. (b) Schematic diagram illustrating the orientations of the variants involved with respect to the foil orientation. (c) BF image. From (c), notice the loop contrast which delineates the shape of a variant plate on its (110) habit plane.

An interesting aspect of the shape of a plate is that it has a pronounced shape anisotropy, yet no apparent faceting. These characteristics are not expected if the chemical interfacial energy of the plate edge is anisotropic or if it is isotropic and makes a dominant contribution to the total shape-dependent energy. In such cases, the shape of a plate would be either polygonal or circular. This leads us to presume that the observed shape may be largely due to another common factor governing the shape of a plate, that is, an elastic energy contribution. In order to test this reasoning and to better understand the details of the observed shape, a calculation was carried out, using the elasticity theory of the shape of a coherent inclusion, developed by Khachaturyan and Hairapetyan (10,11).

For calculating the shape, we first selected two variants, consistent with the convention used in the BF image of Fig. 2: one variant, with its c axis parallel to [100], is taken as the matrix and the other variant with its c axis parallel to [010] as an inclusion. The stress free transformation strain of the inclusion variant, with respect to the matrix variant, is given by

$$\hat{\varepsilon}^o = \begin{pmatrix} \dfrac{a}{c} - 1 & 0 & 0 \\ 0 & \dfrac{c}{a} - 1 & 0 \\ 0 & 0 & 0 \end{pmatrix} \qquad (2)$$

where a and c are the lattice parameters of the $L1_0$ phase. From the SADP of a 48 h aged state, the c/a ratio was measured (0.96) in order to estimate the stress free transformation strain. Since the elastic constants of the Fe-45 at.% Pd alloy are not known, we calculated for two possible bounding ratios of C_{12}/C_{11}, based on the room temperature elastic constants data of the Fe-32.5 at.% Pd disordered alloy, recently measured by Muto et al. (12): $C_{11} \sim 16 \times 10^{10}$ N/m^2, $C_{12} \sim 13.8 \times 10^{10}$ N/m^2 and $C_{44} \sim 7.3 \times 10^{10}$ N/m^2. Fig. 3 shows the results. One can notice that the calculated shapes are in good agreement with the observed shape in two important aspects. First, the calculated shapes correctly reproduce the directions of the long and short axes of the loop-contrast. Since shape-dependent elastic energy is similar to that of a dislocation loop (10), we may take [001] as the direction of low line tension and [110] as that of high line tension. In addition to this, the aspect ratios are found to be fairly close to the experimental values (0.38 ~ 0.5). This clearly demonstrates the importance of the role, played by elastic strain energy, in determining the shape of structual domain plates.

Conclusion

By use of thin specimens of the Fe-45 at.%Pd alloy, we studied the microstructures of the $L1_0$ ordered phase, specifically the morphological features of structural domains, such as variant volume fraction and the shape of a structural domain plate. As for the volume fraction, we observed a characteristic sequential change with the progress of ordering. Initially from the three variant state, the variant volume fraction in a local region was found to vary gradually through the two variant state until a near single variant state was reached. We suggested that this sequential change can be understood in the light of theories of polytwin morphology, by taking into account the ordering characteristics and the limited constraining ability of thin specimen geometry. As to the shape of a structural domain plate, we found that being embedded in the matrix of the other variant, it maintains an elliptic shape, with no faceting. This clearly suggests the importance of elastic strain energy, relative to chemical interfacial energy, in determining the shape of a domain plate. Calculation of the shape, using an elasticity theory, led to good agreement with experimental results.

Acknowledgements

References

1. P. J. Fillingham, H. J. Leamy and L. E. Tanner, *Electron Microscopy and the Structure of Materials,* Univ. of California Press (1972).
2. S. H. Wen, A. G. Khachaturyan, J. W. Morris, Jr., *Metall. Trans.* **12A**, 581 (1981).
3. I. N. Sakahnskaya, Ye. I. Teytel', N. I. Timofeyev, Yu. P. Denisov and P. N. Syutkin, *Fiz. met. metalloved.*,**49**, 363 (1980).
4. H. C. Tong and C. M. Wayman, *Acta metall.*, **21**, 138 (1973).
5. A. G. Khachaturyan and G. A. Shatalov, *Sov. Phys. JETP*, **29**, 557 (1969).
6. A. L. Roitburd, *Sov. Phys. Solid State*, **10**, 2870 (1969).
7. A. L. Roitburd, *Phys. Stat. Sol.* , **16 (a)**, 329 (1973).
8. L. M. Magat, A. S. Yermolenko, G. V. Ivanova, G. M. Makarova and Ya. S. Shur, *Fiz. met. metalloved.*, **26**, 511 (1968).
9. R. Smith , J. S. Bowless, *Acta metall.*, **8**, 405 (1960).
10. A. G. Khachaturyan and V. N. Hairapetyan, *Phys. Stat. Sol.*, **57 (b)**, 801 (1973).
11. A. G. Khachaturyan, *Theory of Structural Transformations in Solids*, John Wiley & Sons, New York (1983).
12. S. Muto, R. Oshima and F. E. Fujita, *Acta metall. mater.*, **38**, 685 (1990).
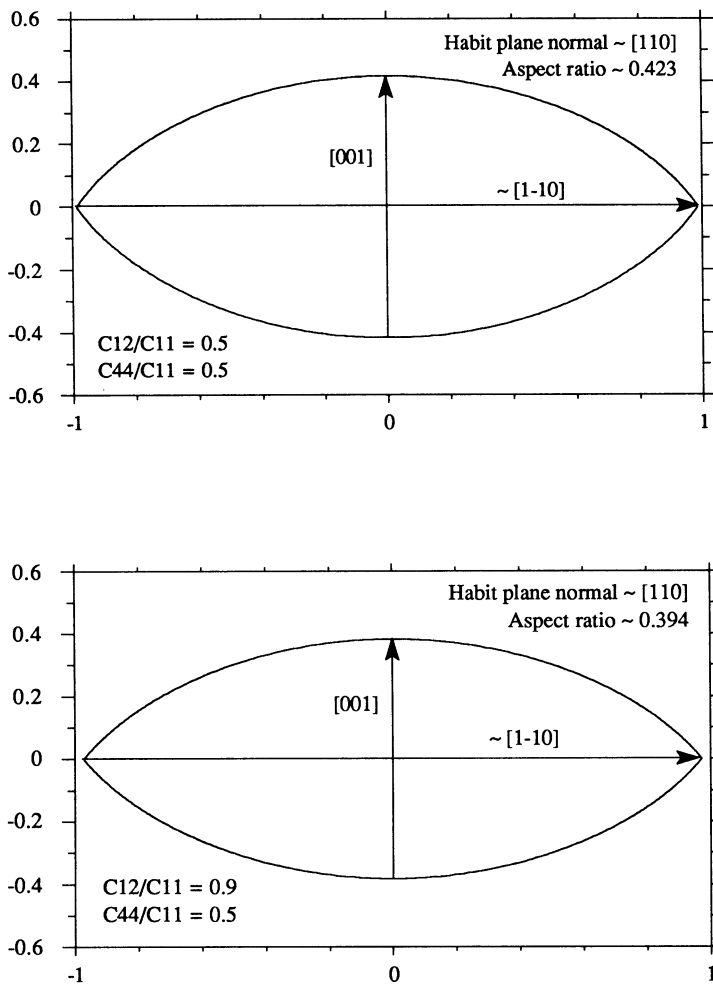
Figure 3: Calculated shapes of a plate-like region of the variant 1 (with c axis parallel to the [100] direction) coherently embedded in a region of the variant 2 (with c axis parallel to the [010] direction). Compare these with the observed shape shown in Fig. 2).